

Organic & Biomolecular Chemistry

Accepted Manuscript



This article can be cited before page numbers have been issued, to do this please use: S. Su, F. Du and Z. Li, *Org. Biomol. Chem.*, 2017, DOI: 10.1039/C7OB02188G.



This is an Accepted Manuscript, which has been through the Royal Society of Chemistry peer review process and has been accepted for publication.

Accepted Manuscripts are published online shortly after acceptance, before technical editing, formatting and proof reading. Using this free service, authors can make their results available to the community, in citable form, before we publish the edited article. We will replace this Accepted Manuscript with the edited and formatted Advance Article as soon as it is available.

You can find more information about Accepted Manuscripts in the [author guidelines](#).

Please note that technical editing may introduce minor changes to the text and/or graphics, which may alter content. The journal's standard [Terms & Conditions](#) and the ethical guidelines, outlined in our [author and reviewer resource centre](#), still apply. In no event shall the Royal Society of Chemistry be held responsible for any errors or omissions in this Accepted Manuscript or any consequences arising from the use of any information it contains.



Journal Name

ARTICLE

Synthesis and pH-dependent hydrolysis profiles of mono- and dialkyl substituted maleamic acids†

Shan Su^a, Fu-Sheng Du^{*a}, and Zi-Chen Li^{*a}

x,
Accepted 00th January 20xx

DOI: 10.1039/x0xx00000x

www.rsc.org/

Maleamic acid derivatives as weakly acid-sensitive linkers or caging groups have been used widely in smart delivery systems. Here we report the controlled synthetic methods to mono- and dialkyl substituted maleamic acids and their pH-dependent hydrolysis behaviors. Firstly, we studied the reaction between n-butylamine and citraconic anhydride, and found that the ratio of the two n-butyl citraconamic acid isomers (α and β) could be finely tuned by controlling the reaction temperature and time. Secondly, we investigated the effects of solvent, basic catalyst, and temperature on the reaction of n-butylamine with 2,3-dimethylmaleic anhydride, and optimized the reaction conditions to efficiently synthesize the dimethylmaleamic acids. Finally, we compared the pH-dependent hydrolysis profiles of four OEG-NH₂ derived water-soluble maleamic acid derivatives. The results reveal that the number, structure, and position of the substituents on the cis-double bond exhibit a significant effect on the pH-related hydrolysis kinetics and selectivity of the maleamic acid derivatives. Interestingly, for the mono-substituted citraconamic acids (α -/ β -isomer), we found that their hydrolyses are accompanied by the isomerization between the two isomers.

Introduction

Smart delivery systems are designed materials that can sense various exogenous or endogenous stimuli such as pH,¹⁻³ light,⁴ redox,⁶⁻⁸ temperature^{9, 10} or enzyme,¹¹⁻¹³ and activate their functions accordingly. The past several decades witnessed rapid growth of preparation and application of smart delivery systems. Acid-sensitive delivery systems represent one of the most concerned smart delivery systems, because pH varies minorly or significantly at the level of cells, tissues, or organs of the human body.^{14, 15} For example, the normal blood pH (7.4) differs from the extracellular pH (6.5-6.8) in most solid tumours or the intracellular endosomal and lysosomal pH (5.0-6.0).¹⁶ A well-designed acid-sensitive delivery system can respond to the minute pH decrease, locates the target areas, and then effectively release bioactive compounds.

Many acid-sensitive delivery systems contain various acid-labile chemical bonds like ketal,¹⁷ imine,^{18, 19} hydrazone,^{20, 21} silyl ether²², and ortho ester.²³⁻²⁵ In 1950s, Bender et al^{26, 27} found that phthalamic acid underwent a fast hydrolysis of the amide at low pH through the intramolecular catalysis of the neighbouring carboxylic acid group. It provided a basis for the development of a new type of acid-labile linkers. Later,

maleamic acids and the mono- or dialkyl substituted derivatives were found to be much more pH-sensitive. Their amide bonds can be hydrolyzed under weakly acidic condition that is physiologically available.²⁸⁻³⁰ Of importance, after the hydrolysis of maleamic acid derivatives, the negatively charged carboxyl acid group is transformed to the positively charged amine group. By virtue of the unique weak acid-sensitivity and charge-conversion, maleamic acid derivatives have been widely used as smart carriers to deliver nucleic acids,³¹⁻³⁴ proteins^{35, 36} and drugs.³⁷⁻³⁹ Although maleamic acid derivatives have been investigated and used as mildly acid-labile linkers or caging groups for many years, limited publications report the influence of molecular structures on the reaction between anhydrides and amines, and on the pH-dependent hydrolysis of the maleamic acid derivatives. The reaction of citraconic anhydride with amine gave a mixture of two isomers with different positional substituents that may influence the hydrolysis of the amide bond.^{40, 41} However, it has not been reported how to control the ratio of the two isomers. Moreover, because of the lower ring strain of the di-substituted maleic anhydrides, their reaction rates with amine were much slower than those of the mono-substituted ones.⁴² The di-substituted maleamic acid was usually obtained by the ineffective reaction of amine with excessive di-substituted maleic anhydride, resulting in the poor atom economy and the difficulty of product isolation.^{43, 44} Previous studies focused on the hydrolysis mechanism and the relationship between structure and hydrolysis rate of maleamic acid derivatives,^{27, 44-47} however, the hydrolysis selectivity at different pH—an

^a Beijing National Laboratory for Molecular Sciences (BNLMS), Key Laboratory of Polymer Chemistry & Physics of Ministry of Education, Department of Polymer Science & Engineering, College of Chemistry and Molecular Engineering, Peking University, Beijing 100871, China.

E-mail: fsdu@pku.edu.cn (F. S. Du); zcli@pku.edu.cn (Z. C. Li)

†Electronic Supplementary Information (ESI) available: Additional NMR spectra and MS spectra. See DOI: 10.1039/x0xx00000x

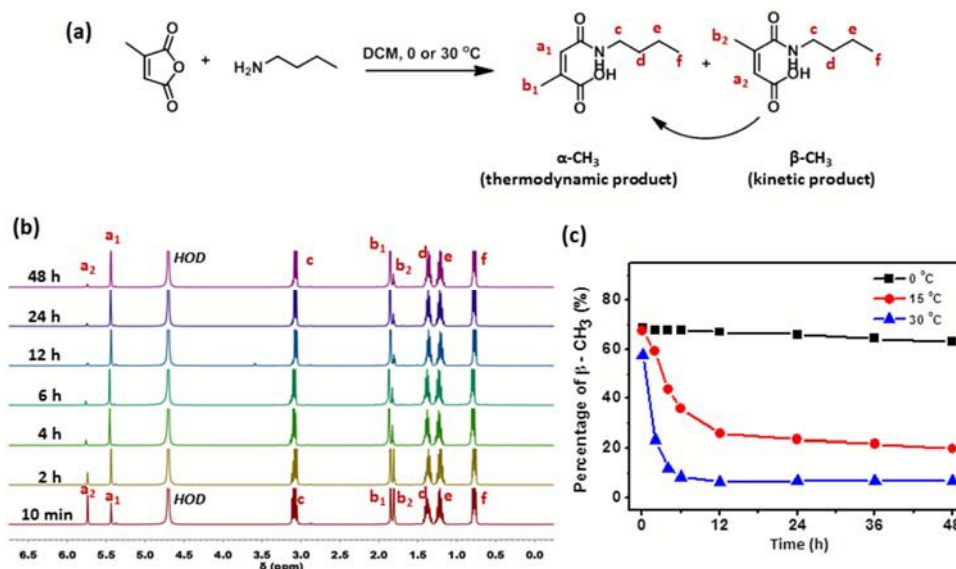


Fig. 1 (a) Formation and isomerization of n-butyl citraconamic acid (α -CH₃/ β -CH₃). (b) ¹H NMR spectra of the isomerization of n-butyl citraconamic acids at 30 °C; (c) Tautomerization kinetics of β -CH₃ to α -CH₃ citraconamic acid at different temperature.

important factor for smart nanomedicine—has not been systematically studied. Herein, we report the simple methods to control the ratio of two positional isomers of the mono-substituted maleamic acids, and a highly efficient way to synthesize the di-substituted maleamic acids. In addition, we systematically studied the hydrolysis profiles of mono- or di-substituted maleamic acids to elucidate their hydrolysis selectivity towards various physiologically available pH.

Results and discussion

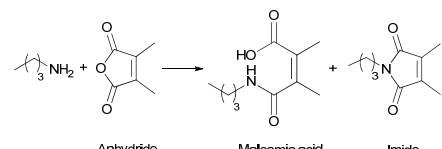
Isomerization of mono-substituted maleamic acid

The nucleophilic addition of primary amine to citraconic anhydride produced two citraconamic acid isomers, α -CH₃ and β -CH₃ as shown in Fig. 1a. Baydar and Scheeren reported that α -CH₃ is the thermodynamic product and β -CH₃ is the kinetic one. At high temperatures, β -CH₃ tends to rearrange into the more stable α -CH₃.^{40, 41} To study the isomerization kinetics of citraconamic acid, we performed the reaction of citraconic anhydride and n-butylamine at different temperature (0 °C, 15 °C and 30 °C). The reaction rate was extremely fast with complete consumption of the reactants within 10 min even at 0 °C. Time-dependent ¹H NMR measurements were carried out to determine the isomerization kinetics of from β -CH₃ to α -CH₃ (Fig. 1b). It was found that both isomers were formed initially, however, the signals of the β -CH₃ isomer decreased gradually while those of the α -CH₃ isomer increased with time. The percentage of the β -CH₃ isomer in the mixture of the two isomers was determined by comparing the integrals of peaks a₁ and a₂, and plotted against time (Fig. 1c). At 0 °C, the percentage of the β -CH₃ isomer decreased very slowly from the initial 69% to 64% in 48 h. When the reaction temperature was raised to 15 °C and 30 °C, the initial content of the β -CH₃ isomer did not change much, being 67% and 58% respectively.

This indicates that the reaction temperature exerted little effect on the initial ratio of the two isomers under the used experimental conditions. In contrast, the intramolecular isomerization rate from β -CH₃ to α -CH₃ increased rapidly with increasing temperature. After 48 h, the final percentage of the β -CH₃ isomer decreased to 20 % at 15 °C and 7% at 30 °C, respectively. On the whole, the ratio of the two isomers can be controlled by reaction temperature and time. Higher temperature and longer reaction time favor the α -CH₃ isomer over β -CH₃. In addition, no Michael addition products from amine and anhydride were detected as evidenced by the NMR spectra.

Optimization of the synthetic parameters for the di-substituted maleamic acid

The reaction of di-substituted maleic anhydride and a primary amine produces a mixture of maleamic acid and maleimide. The attempt to purify the maleamic acid was unsuccessful due to the spontaneous tendency to cyclization.^{48, 49} Although a number of papers report the formation of di-substituted maleamic acids as acid-labile linkers or caging groups, none of them gave detailed information about the reactions between di-substituted maleic anhydride and amines.^{34, 50} Herein, the reactions of n-butylamine and 2,3-dimethylmaleic anhydride were carried out under various conditions to study the effects of solvent, basic catalyst, and reaction temperature on the conversion of reactants and the ratio of the two isomeric products, n-butyl dimethylmaleamic acid and n-butyl dimethylmaleimide (Fig. S1 and Table 1). We found that more maleamic acid was produced in DMF than in less polar THF. Pyridine did not show obvious effect to increase the ratio of maleamic acid over maleimide. However, when TEA was used, either the conversion of the anhydride or the percentage of n-butyl dimethylmaleamic acid was raised significantly (Table 1). We assumed that the more basic TEA could effectively promote the nucleophilic addition reaction of

Table 1 Effects of solvent and basic catalyst on the reaction of n-butyl amine and 2, 3-dimethylmaleic anhydride^a


Entry	Solvent	Base	Anhydride (%)	Maleamic acid (%)	Imide (%)
1	THF	none	28	27	45
2	THF	Py	21	32	47
3	THF	TEA	13	65	22
4	DMF	none	27	46	26
5	DMF	Py	30	44	26
6	DMF	TEA	5	85	10

^a Determined by ¹H NMR spectra. Concentration of reactant: 1.0 mol/L, molar ratio of catalyst/anhydride: 1.0, 30 °C, 4 h. TEA = triethylamine, Py = pyridine.

Table 2 Effects of TEA amount on the reaction of n-butyl amine and 2, 3-dimethylmaleic anhydride^a

Entry	Base equiv.	Anhydride (%)	Maleamic acid (%)	Imide (%)
1	0.5	19	81	0
2	1.0	8	92	0
3	2.0	2	98	0
4	3.0	1	99	0

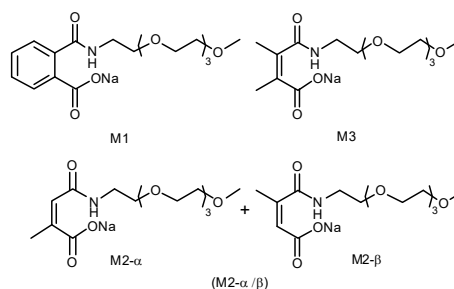
^a Determined by ¹H NMR spectra. Concentration of reactant: 1.0 mol/L in DMF, 0 °C, 4 h.

amine toward anhydride and neutralize the *in situ* generated carboxylic acid, thus preventing the formation of imide by-product *via* dehydration of maleamic acid.

Based on the above results, we further carried out the reaction in DMF at 0 °C using TEA as the catalyst. As shown in Table 2, the low temperature (0 °C) could effectively inhibit the formation of the imide by-product. The molar ratio of TEA also had a significant effect on the conversion of the reactants. When the molar ratio of TEA to anhydride was less than or equal to 1.0, the conversion could not reach 100 %. With increasing the ratio of TEA/anhydride to 2.0 or more, almost all of the anhydride was consumed in 4 h. On the whole, we found the optimal condition for the synthesis of alkyl dimethylmaleamic acid without the formation of the imide by-product. Compared to similar reactions in previous reports where excessive anhydrides are necessary, this optimal condition is highly efficient with good atom economy.

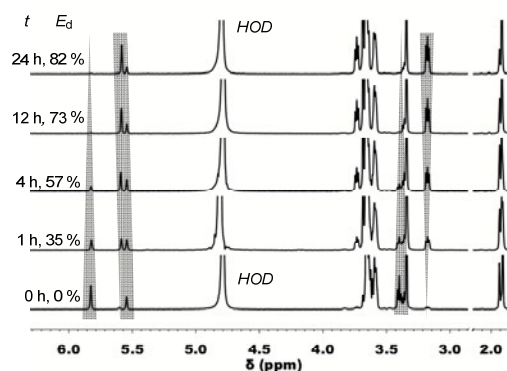
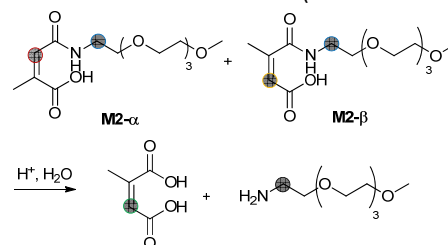
pH-Dependent hydrolysis

The structure of the substituents greatly influences the acid-catalyzed hydrolysis kinetics of maleamic acid derivatives.^{44, 45} To study the physiologically available pH-dependent hydrolysis behaviors, four maleamic acid derivatives were synthesized from the corresponding anhydrides and OEG₄-NH₂ via the above optimized conditions (Scheme 1 and S1). The reaction of

**Scheme 1** Structure of compounds **M1**, **M2-α**, **M2-β** and **M3**.

citraconic anhydride and OEG₄-NH₂ produced a mixture of two isomers, **M2-α** and **M2-β**. Since **M2-α** and **M2-β** underwent rapid tautomerization, isolation and purification of the two isomers by thin layer, column chromatography or HPLC failed. However, the ratio of **M2-α** to **M2-β** could be tuned by changing the reaction temperature. We prepared two **M2** samples with different isomer ratios, **M2-94/6** ($\alpha/\beta = 94/6$) and **M2-33/67** ($\alpha/\beta = 33/67$), by performing the reaction at 30 °C for 24 h and 0 °C for 1 h, respectively. All the samples were stored in the form of sodium salt in order to avoid the plausible isomerization or pre-hydrolysis. Their structures were confirmed by ¹H/¹³C NMR and ESI-MS spectra (Fig. S3-S10).

The hydrolysis profiles of the four samples were studied by ¹H NMR at various pH (5.5, 6.5, or 7.4, 37 °C). Although phthalamic acid (**M1**) could be hydrolysed quickly *via* the intramolecular catalysis mechanism at pH 3 or lower, it was reasonably stable in the weakly acidic aqueous media.²⁷ At pH 5.5, only 4.6 % of the **M1** was hydrolyzed in 3 d (Fig. S11). No hydrolysis was observed after incubation for 12 d at pH 7.4. The mono-substituted maleamic acids (**M2-α** and **M2-β**) are

**Fig. 2** ¹H NMR spectra of **M2-33/67** monitored during the hydrolysis process in buffered D₂O (pH 5.5) at 37 °C. The detailed assignment of the proton signals is shown in Fig. S12. The sample was used in the form of sodium salt.

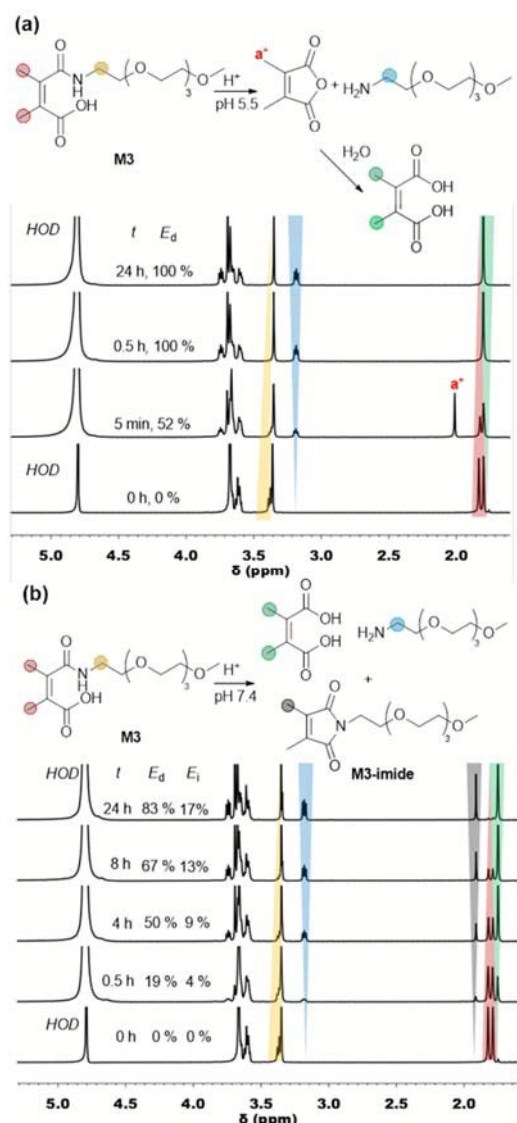


Fig. 3 ¹H NMR spectra of **M3** monitored during the hydrolysis process at pH 5.5 (a) and pH 7.4 (b), 37 °C. The detailed ¹H NMR spectrum is shown in Fig. S15 and Fig. S17. The sample was used in the form of sodium salt.

much more acid-sensitive than **M1**. At pH 5.5, both the **M2** samples could be hydrolyzed to citraconic acid and OEG₄-NH₂ efficiently, reaching a hydrolysis degree of 82% for **M2-33/67**

and 76 % for **M2-94/6**, respectively in 24 h (Fig. 2 and Fig. S13). Interestingly, the position of the methyl group exhibited a significant effect on the hydrolysis of the amide bond. As shown in Fig. 2, **M2-β** was hydrolyzed much faster than **M2-α**. Eventually, both samples were hydrolyzed completely to citraconic acid and OEG₄-NH₂ as proven by the mass spectrum of the final hydrolysis products (Fig. S14).

The di-substituted maleamic acid (**M3**) is the most sensitive one toward hydrolysis. Upon incubation in weakly acidic aqueous solution (pH 5.5), **M3** was hydrolyzed quickly, reaching a hydrolysis degree of 52% in 5 min. The hydrolysis finished within 0.5 h, producing 2,3-dimethylmaleic acid and OEG₄-NH₂ (Fig. 3a). We could see the methyl signal (2.01 ppm) of the transient 2,3-dimethylmaleic anhydride during the hydrolytic process because **M3** was hydrolyzed faster than the intermediate anhydride.⁴⁵ The hydrolysis profile of **M3** at pH 6.5 was similar to that at pH 5.5 but with a lower rate (Fig. S16). **M3** was not stable even at pH 7.4, and was hydrolyzed completely in 24 h (Fig. 3b). Notably, under the neutral condition, **M3** was not hydrolyzed completely to 2,3-dimethylmaleic acid and OEG₄-NH₂. 17% of **M3** was converted into the imide that was not observed in the weakly acidic media (Fig. 3b and S17). All the hydrolysis products were further confirmed by ESI-MS (Fig. S18-S20).

Fig. 4 shows the hydrolysis kinetic curves of the four samples at different pHs. The hydrolysis rates follow an order of **M3** >> **M2-33/67** > **M2-94/6** >> **M1** under the same condition. From these curves, the half-life times ($t_{1/2}$) of the amide hydrolysis could be determined. We also calculated the ratio of $t_{1/2}$ at pH 7.4 ($t_{1/2-7.4}$) to that of pH 5.5 ($t_{1/2-5.5}$), which was applied to judge the pH-related hydrolysis selectivity of **M1-M3** (Table 3). The larger ratio represents the better selectivity toward hydrolysis. Wagner and co-workers proposed that if the ratio of $t_{1/2-7.4}$ to $t_{1/2-5.5}$ of an acid-labile bond or chemical structure is larger than 15, it can be deemed as the highly selective one toward hydrolysis.⁵¹ As aforementioned, **M1** was stable against hydrolysis in neutral buffer solution and its hydrolysis $t_{1/2}$ was larger than 6 months even at pH 5.5. It is not an appropriate weak acid-sensitive linker or caging group. In contrast, the other compounds are highly sensitive to the physiologically available, weakly acidic media and show excellent hydrolysis selectivity. Particularly,

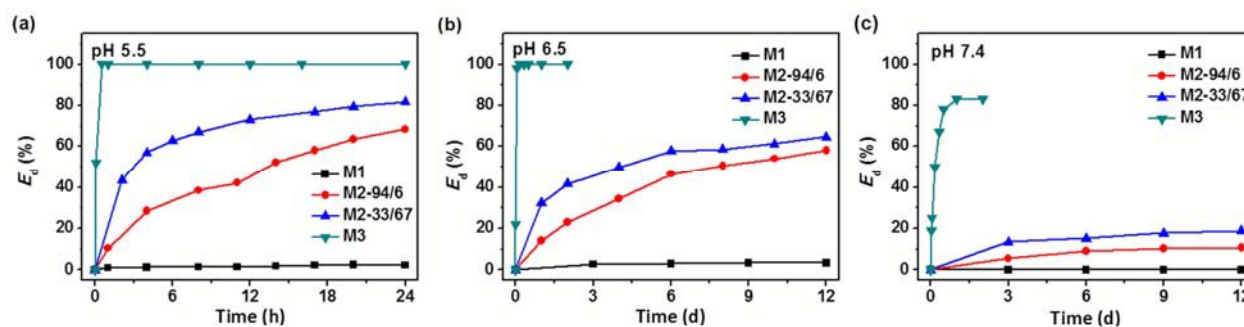


Fig. 4 Hydrolysis kinetics of **M1**, **M2-94/6**, **M2-33/67** and **M3** at various pH values.

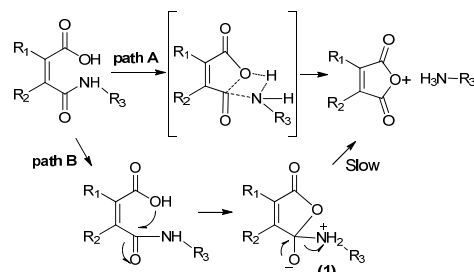
Table 3 The hydrolysis half-life time $t_{1/2}$ at various pH values.

Entry	$t_{1/2}$ at varied pH			Ratio of $t_{1/2-7.4}/t_{1/2-5.5}$
	pH 5.5	pH 6.5	pH 7.4	
M1	- ^a	- ^a	- ^a	-
M2-94/6	13.3 h	8.1 d	187 d	337
M2-33/67	3.3 h	4.2 d	145 d	1054
M3	0.08 h	0.37 h	3.8 h	47.5

^a Hydrolysis did not reach 50 % after 6 months.

M2-33/67 possesses the best selectivity with the ratio of $t_{1/2-7.4}$ to $t_{1/2-5.5}$ being 1054. Though the hydrolysis selectivity of the most acid-sensitive **M3** is not as good as **M2-33/67** or **M2-94/6**, a ratio of $t_{1/2-7.4}$ to $t_{1/2-5.5}$ for **M3** was measured to be 47.5, being much larger than 15.

According to the aforementioned results, we conclude that the substituents on the carbon-carbon double bond greatly influence the pH-dependent hydrolysis kinetics and selectivity of the maleamic acid derivatives. The acid sensitivity decreases in the order of **M3** >> **M2- β** > **M2- α** >> **M1**, and the hydrolysis selectivity follows the order of **M2- β** > **M2- α** > **M3**. The effect of the substituents can be attributed to the intramolecular catalysis mechanism of the amide hydrolysis by the neighbouring carboxylic acid group via a concerted process.^{27, 46, 47} In this process, the proton transfer from hydroxyl oxygen to amidic nitrogen, the formation of new C-O bond and C-N bond cleavage occur simultaneously (Scheme 2, path A). Although Kirby and Lancaster proposed a multi-step hydrolysis mechanism and assumed that the elimination of the amine was the rate-determining step (Scheme 2, path B), they did not provide convincing evidences.⁴⁵ Given the correctness of their proposal, the tetrahedral intermediate (**1**) should be detected

**Scheme 2** Plausible hydrolysis mechanism of the maleamic acid derivatives.

easily. However, we did not observe any of the signals assignable to this tetrahedral intermediate during the hydrolysis process of the substituted maleamic acids. Considering the concerted intramolecular mechanism, the dialkyl substituents on the *cis*-double bond can accelerate the cyclization reaction because of the *gem*-dialkyl effect (Thorpe-Ingold effect).⁴² The steric hindrance of the substituents results in a compression of the internal angle between the amide and carboxylic acid groups. Consequently, the two reactive groups move closer and the intramolecular attack is more effective. This justifies why **M3** was hydrolyzed much faster than **M2**. Once the two substituents on the double bond form a ring, in particular an aromatic ring which is conformationally unfavourable for the two reactive groups getting closer, the intramolecular hydrolysis rate will be dramatically reduced. Therefore, **M1** shows the lowest hydrolysis rate. These findings are in good agreement with the previous reports.^{44, 45}

Hydrolysis kinetics of **M2- α** and **M2- β**

In the previous section, we noticed that **M2- β** was hydrolysed faster than **M2- α** (Fig. 2). Lynn et al⁵² also found similar phenomenon for the hydrolysis of the poly(allylamine) derivatives with pendent citraconamic acid groups. However, the polymeric effect of polyelectrolytes may complicate the pH-dependent hydrolysis kinetics of the amide bonds.

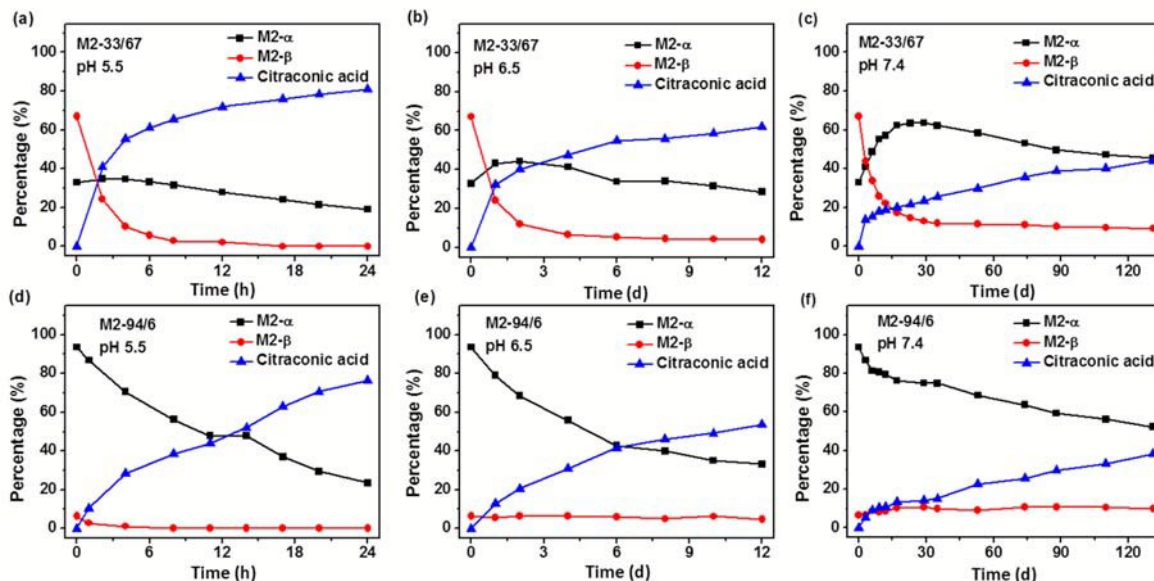
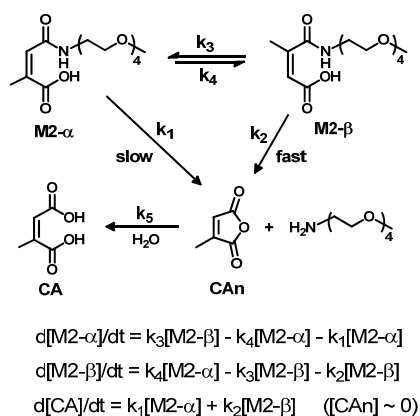


Fig. 5 The content change curves of **M2- α** , **M2- β** and citraconic acid of **M2-33/67** (a-c) or **M2-94/6** (e-f) at various pH value. The percentages of **M2- α** , **M2- β** and citraconic acid are determined by comparing the peak integrals of the olefinic groups of the three compounds in the ¹H NMR.



Scheme 3 Plausible mechanism of hydrolysis and isomerization of **M2-α** and **M2-β** in deuterated phosphate buffer. **[M2-α]**, **[M2-β]**, **[CA]** and **[CAn]** denote the temporal concentration of **M2-α**, **M2-β**, **CA** and **CAn**, respectively, during the hydrolysis/tautomerization process.

To better understand the effect of substituted position on the hydrolysis kinetics of citraconamic acid isomers, we studied the hydrolysis profiles of **M2-α** and **M2-β** in detail by monitoring separately the proton signals of **M2-α** and **M2-β** in the two samples (**M2-33/67** and **M2-94/6**) at different pHs (Fig. 5).

In the case of **M2-33/67** at pH 5.5 (Fig. 5a), the percentage of **M2-β** declined quickly from the initial 67% to 10% in the first 4 h, beyond which it decreased gradually to 0 in 17 h. In contrast, at the same initial stage (4 h), the amount of **M2-α** increased slightly from 33% to 35%. After this maximum point, it decreased slowly to 20% in 24 h. These results could be attributed to the concurrent hydrolysis of the two isomers and their isomerization to each other as shown in Scheme 3. At pH 5.5, in the initial period (0-4 h), the isomerization rate from **M2-β** to **M2-α** was higher than the hydrolysis rate of **M2-α** ($d[M2-\alpha]/dt > 0$). With the fast hydrolysis of **M2-β**, after 4 h, $d[M2-\alpha]/dt$ became negative. Therefore, there exists a maximum point. When the pH was raised to 6.5, both k_1 and k_2 would be decreased with a larger magnitude than k_3 or k_4 , causing the more obvious maximum point (from 33% to 45%) at the longer time point of 48 h. At pH 7.4, k_1 became small enough to make the hydrolysis rate of **M2-α** lower than the isomerization rate from **M2-β** to **M2-α** within 20 d. The percentage of **M2-α** did not decline but increase from the initial 33% to 64% until 23 d, beyond which it decreased slowly to 45% in 130 d. We did not detect the proton signal of the intermediate citraconic anhydride (CAn) in the hydrolysis process, indicating that the hydrolysis rate of CAn was much higher than that of **M2-α/β** ($k_5[H_2O] \gg k_1[M2-\alpha] + k_2[M2-\beta]$) at all the used pHs.

For sample **M2-94/6**, the percentage of **M2-α** decreased monotonously at all the pHs, without the maximum point as observed for **M2-33/67**. This means that $d[M2-\alpha]/dt$ was negative (< 0), which can be attributed to the low initial concentration of **M2-β** in the system. As expected, the hydrolysis rate of **M2-α** decreased significantly with increasing pH (Figs. 5d-5f). It is noticed that at pH 6.5, the percentage of **M2-β** remained almost constant (5%) within 12 h. This

indicates that the isomerization rate from **M2-α** to **M2-β** was approximately equal to the hydrolysis rate of **M2-β**, that is $d[M2-\beta]/dt \approx 0$. Similarly, for sample **M2-33/67**, a dynamic equilibrium was also established after a rapid decrease in percentage of **M2-β**, reaching the same constant value (5%). Moreover, at pH 7.4, another dynamic equilibrium was obtained with the constant **M2-β** percentage of 9% in the period of 30-130 d.

Conclusion

By studying the nucleophilic addition reaction of a primary amine toward citraconic or 2,3-dimethylmaleic anhydride, we demonstrate the optimized conditions to control the ratio of two positional isomers (α and β) of alkyl citraconamic acids and to prepare the alkyl dimethylmaleamic acid derivatives with good atom economy. Four water-soluble maleamic acid derivatives have been prepared from OEG-NH₂ by reacting with different anhydrides. These compounds show the pH-dependent hydrolysis behaviours via an intramolecular catalysis mechanism: amide attacked by the neighbouring carboxylic acid group in a concerted process. The hydrolysis kinetics is greatly influenced by the number, structure, and position of the substituents on the double bond, and the acid-sensitivity decreases in the order of di-substituted **M3** \gg mono-substituted **M2-β** isomer $>$ mono-substituted **M2-α** isomer \gg aromatic ring-fused **M1**. The citraconamic acid and 2,3-dimethylmaleamic acid derivatives (**M2-α**, **M2-β**, **M3**) are extremely sensitive toward physiologically available acidic environment and show excellent hydrolysis selectivity—a key parameter to be considered when used as the acid-sensitive linkers or caging groups for smart nanomedicines. Moreover, the complex hydrolysis kinetic curves for the mono-substituted citraconamic acids imply the concurrent hydrolysis and mutual isomerization of α - and β -isomers. On the whole, the acid-sensitivity and hydrolysis selectivity of the alkyl maleamic acid derivatives can be easily tuned by changing the number, structure and position of the substituents on the *cis*-double bond, aiding design of various acid-labile moieties for application in different smart delivery systems.

Experimental section

General

Phthalic anhydride (98 %, Alfa Aesar), citraconic anhydride (99 %, J&K Chemical Ltd), 2,3-dimethylmaleic anhydride (96 %, J&K Chemical Ltd), 3,6,9,12-tetraoxatridecylamine (OEG₄-NH₂, 98 %, Beijing Isomersyn Technology Co., Ltd) were used as received. Deuterated phosphate buffer (PB) solution with pH 7.4, 6.5 and 5.5 was prepared from NaOD (40 wt% in D₂O, Alfa) and deuterated phosphoric acid (85 wt% in D₂O, Alfa). Other reagents were purchased from Beijing Chemical Reagent Co. and used without further purification. ¹H NMR and ¹³C NMR spectra were recorded on a Bruker ARX 400 MHz spectrometer. Electrospray ionization mass spectroscopy (ESI-MS) measurements of **M1-M3** were performed on a Bruker

APEX-IV Fourier transform mass spectrometer. Mass spectroscopy (MS) of the hydrolysis products was performed on a quadrupole rods SQ Detector 2 mass spectrometer (Waters Corporation) in positive and negative ion modes, respectively.

Synthesis and isomerization of n-butyl citraconamic acids

n-Butyl amine (1.0 mmol) and citraconic anhydride (1.0 mmol) were added in anhydrous dichloromethane (DCM, 2.0 mL). The reaction mixture was stirred at 0 °C. ¹H NMR was recorded at specific time point. The ratio of the α-CH₃ isomer and the β-CH₃ isomer was estimated by the ¹H NMR spectra. By changing the temperature from 0 °C to 15 °C or 30 °C, the samples with different ratios of the two isomers could be obtained. Also, the isomerization experiments at different temperatures were carried out following the same procedure.

Optimization of the synthetic condition of n-butyl-2,3-dimethylmaleamic acid

n-Butyl amine (1.0 mmol) and 2,3-dimethylmaleic anhydride (1.0 mmol) were added in anhydrous tetrahydrofuran (THF, 2.0 mL). The reaction mixture was stirred at 30 °C for 4 h. After removing THF, the residue was measured by ¹H NMR to determine the amount of various compounds in the mixture. Similar procedure was used for other experimental conditions, but the solvent was not removed when using DMF as the solvent.

Syntheses of M1-M3

Phthalamic acid (M1)

Phthalic anhydride (1.0 mmol) and mOEG₄-NH₂ (1.0 mmol) were added in anhydrous DCM (2.0 mL) at ambient temperature. After stirring for 1 h, the mixture was concentrated on a rotary evaporator. The concentrated product was added into a 1 N NaHCO₃ solution (1.2 equiv.) and lyophilized. **M1** was obtained as a white solid (yield: >99 %). ¹H NMR (400 MHz, D₂O, ppm): δ 7.57 (dd, *J* = 7.4, 1.5 Hz, 1H), 7.52-7.40 (m, 3H), 3.71-3.51 (m, 16H), 3.29 (s, 3H). ¹³C NMR (101 MHz, D₂O, ppm): δ 75.8, 173.0, 164.2, 137.5, 134.3, 130.3, 129.4, 128.0, 127.1, 70.9, 69.5, 69.5, 69.4, 69.4, 69.3, 68.7, 58.0, 39.4. ESI-MS: calcd for C₁₇H₂₄NO₇ [M-H]⁻ 354.154189; found 354.154729.

Citraconamic acids (M2-α/β)

Synthesis of **M2-α/β** followed the same procedure as for **M1**, except that the reaction temperature and time were changed to 30 °C, 24 h (for **M2-94/6**) or 0 °C, 1 h (for **M2-33/67**). **M2-94/6** and **M2-37/6** were obtained as white solids after lyophilization (yield > 99 %). ¹H NMR (400 MHz, D₂O, ppm): for **M2-94/6**, δ 5.88 (M2-β, q, *J* = 1.6 Hz, 0.06H), 5.59 (M2-α, q, *J* = 1.6 Hz, 0.94H), 3.75-3.61 (m, 14H), 3.47-3.37 (m, 5H), 1.99 (M2-β, d, *J* = 1.6 Hz, 2.82H), 1.95 (M2-α, d, *J* = 1.6 Hz, 0.18H); for **M2-33/67**, δ 5.88 (M2-β, q, *J* = 1.6 Hz, 0.67H), 5.59 (M2-α, q, *J* = 1.6 Hz, 0.33H), 3.75-3.61 (m, 14H), 3.47-3.37 (m, 5H), 1.99 (M2-α, d, *J* = 1.6 Hz, 0.99H), 1.95 (M2-β, d, *J* = 1.6 Hz, 2.01H). ¹³C NMR (101 MHz, D₂O): for **M2-94/6**, δ 178.7, 167.5, 150.5, 115.7, 71.0, 69.6, 69.5, 69.4, 69.0, 58.0, 38.7, 20.7; for

M2-33/67, δ 178.7, 173.9, 173.4, 167.5, 150.5, 141.3, 126.8, 115.7, 71.0, 69.6, 69.5, 69.4, 69.0, 68.6, 58.0, 39.0, 38.7, 20.7, 19.9. ESI-MS (**M2-94/6**): calcd for C₁₄H₂₄NO₇ [M-H]⁻ 318.153798; found 318.155826. ESI-MS (**M2-33/67**): calcd for C₁₄H₂₄NO₇ [M-H]⁻ 318.155826; found 318.154729.

2,3-Dimethyl maleamic acid (M3)

2,3-Dimethylmaleic anhydride (1.0 mmol), OEG₄-NH₂ (1.0 mmol), and TEA (2.2 equiv.) were added in anhydrous DMF (2.0 mL) at 0 °C. After stirring for 1 h, 1 M NaHCO₃ solution (1.2 equiv.) was added to the mixture. The mixture was concentrated on a rotary evaporator. **M3** was obtained as a white solid (yield > 99 %). ¹H NMR (400 MHz, D₂O, ppm): δ 3.70-3.65 (m, 10H), 3.64-3.56 (m, 4H), 3.38 (t, *J* = 5.2 Hz, 2H), 3.36 (s, 3H), 1.83 (s, 3H), 1.80 (s, 6H). ¹³C NMR (101 MHz, D₂O, ppm): δ 178.3, 174.3, 164.9, 137.8, 127.9, 70.9, 69.6, 69.5, 69.5, 69.4, 68.6, 58.0, 39.0, 36.9, 31.3, 15.5, 14.5. ESI-MS: calcd for C₁₅H₂₆NO₇ [M-H]⁻ 332.170333; found 332.170379.

Hydrolysis kinetics measured by ¹H NMR

Each maleamic acid derivative (1 mg, sodium salt) was dissolved in 500 μL of PB (50 mM, pH 5.5 or 6.5 or 7.4) in a NMR tube. The NMR tubes were incubated at 37 °C, and the ¹H NMR spectrum was recorded at specific time point.

Acknowledgements

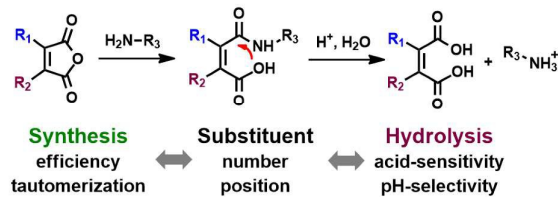
This work was financially supported by the National Key Research and Development Program of China (No. 2016YFA0201400) and National Natural Science Foundation of China (No. 21534001).

Notes and references

- D. Ling, W. Park, S. J. Park, Y. Lu, K. S. Kim, M. J. Hackett, B. H. Kim, H. Yim, Y. S. Jeon, K. Na and T. Hyeon, *J. Am. Chem. Soc.*, 2014, **136**, 5647-5655.
- R. Xu, G. Zhang, J. Mai, X. Deng, V. Segura-Ibarra, S. Wu, J. Shen, H. Liu, Z. Hu, L. Chen, Y. Huang, E. Koay, Y. Huang, J. Liu, J. E. Ensor, E. Blanco, X. Liu, M. Ferrari and H. Shen, *Nat. Biotechnol.*, 2016, **34**, 414-418.
- W. Sun, T. Jiang, Y. Lu, M. Reiff, R. Mo and Z. Gu, *J. Am. Chem. Soc.*, 2014, **136**, 14722-14725.
- Y. Zhang, Q. Yin, L. Yin, L. Ma, L. Tang and J. Cheng, *Angew. Chem., Int. Ed.*, 2013, **52**, 6435-6439.
- N. Fomina, C. McFearin, M. Sermsakdi, O. Edigin and A. Almutairi, *J. Am. Chem. Soc.*, 2010, **132**, 9540-9542.
- X. Liu, J. Xiang, D. Zhu, L. Jiang, Z. Zhou, J. Tang, X. Liu, Y. Huang and Y. Shen, *Adv. Mater.*, 2016, **28**, 1743-1752.
- Y. Ma, Y. Li, H. P. Xu, Z. Q. Wang and X. Zhang, *J. Am. Chem. Soc.*, 2010, **132**, 442-443.
- F. H. Meng, W. E. Hennink and Z. Y. Zhong, *Biomaterials*, 2009, **30**, 2180-2198.
- B. P. Timko, M. Arruebo, S. A. Shankarappa, J. B. McAlvin, O. S. Okonkwo, B. Mizrahi, C. F. Stefanescu, L. Gomez, J. Zhu,

- A. Zhu, J. Santamaria, R. Langer and D. S. Kohane, *Proc. Natl. Acad. Sci. U. S. A.*, 2014, **111**, 1349-1354.
10. J. Akimoto, M. Nakayama and T. Okano, *J. Controlled Release*, 2014, **193**, 2-8.
11. Z. Gu, M. Yan, B. Hu, K.-I. Joo, A. Biswas, Y. Huang, Y. F. Lu, P. Wang and Y. Tang, *Nano Lett.*, 2009, **9**, 4533-4538.
12. A. Biswas, K. Joo, J. Liu, M. X. Zhao, G. P. Fan, P. Wang, Z. Gu and Y. Tang, *ACS Nano* 2011, **5**, 1385-1394.
13. C. E. Callmann, C. V. Barback, M. P. Thompson, D. J. Hall, R. F. Mattrey and N. C. Gianneschi, *Adv. Mater.*, 2015, **27**, 4611-4615.
14. S. Ganta, H. Devalapally, A. Shahiwala and M. Amiji, *J. Controlled Release*, 2008, **126**, 187-204.
15. W. W. Gao, J. M. Chan and O. C. Farokhzad, *Mol. Pharm.*, 2010, **7**, 1913-1920.
16. Y. G. Wang, K. J. Zhou, G. Huang, C. Hensley, X. N. Huang, X. P. Ma, T. Zhao, B. D. Sumer, R. J. DeBerardinis and J. M. Gao, *Nat. Mater.*, 2014, **13**, 204-212.
17. E. R. Gillies, T. B. Jonsson and J. M. J. Frechet, *J. Am. Chem. Soc.*, 2004, **126**, 11936-11943.
18. Y. Jia, J. Fei, Y. Cui, Y. Yang, L. Gao and J. Li, *Chem. Commun.*, 2011, **47**, 1175-1177.
19. Y. L. Zhao, Z. X. Li, S. Kabehie, Y. Y. Botros, J. F. Stoddart and J. I. Zink, *J. Am. Chem. Soc.*, 2010, **132**, 13016-13025.
20. Y. Bae, S. Fukushima, A. Harada and K. Kataoka, *Angew. Chem., Int. Ed.*, 2003, **42**, 4640-4643.
21. C. C. Lee, E. R. Gillies, M. E. Fox, S. J. Guillaudeau, J. M. Frechet, E. E. Dy and F. C. Szoka, *Proc. Natl. Acad. Sci. U. S. A.*, 2006, **103**, 16649-16654.
22. M. C. Parrott, J. C. Luft, J. D. Byrne, J. H. Fain, M. E. Napier and J. M. DeSimone, *J. Am. Chem. Soc.*, 2010, **132**, 17928-17932.
23. R. P. Tang, N. Palumbo, W. H. Ji and C. Wang, *Biomacromolecules*, 2009, **10**, 722-727.
24. S. Lin, F. S. Du, Y. Wang, S. P. Ji, D. H. Liang, L. Yu and Z. C. Li, *Biomacromolecules*, 2008, **9**, 109-115.
25. J. Barr, K. W. Woodburn, S. Y. Ng, H. R. Shen and J. Heller, *Adv. Drug Delivery Rev.*, 2002, **54**, 1041-1048.
26. M. L. Bender, *J. Am. Chem. Soc.*, 1957, **79**, 1258-1259.
27. M. L. Bender, Y. L. Chow and F. Chloupek, *J. Am. Chem. Soc.*, 1958, **80**, 5380-5384.
28. D. B. Rozema, K. Ekena, D. L. Lewis, A. G. Loomis and J. A. Wolff, *Bioconjugate Chem.*, 2003, **14**, 51-57.
29. J. Reményi, B. Balázs, S. Tóth, A. Falus, G. Tóth and F. Hudecz, *Biochem. Biophys. Res. Commun.*, 2003, **303**, 556-561.
30. W. C. Shen and H. J. P. Ryser, *Biochem. Biophys. Res. Commun.*, 1981, **102**, 1048-1054.
31. M. Meyer, C. Dohmen, A. Philipp, D. Kiener, G. Maiwald, C. Scheu, M. Ogris and E. Wagner, *Mol. Pharm.*, 2009, **6**, 752-762.
32. S. T. Guo, Y. Y. Huang, Q. Jiang, Y. Sun, L. D. Deng, Z. C. Liang, Q. Du, J. F. Xing, Y. L. Zhao, P. C. Wang, A. Dong and X. J. Liang, *ACS Nano* 2010, **4**, 5505-5511.
33. L. Han, C. Tang and C. Yin, *Biomaterials*, 2015, **44**, 111-121.
34. Y. Li, J. Yang, B. Xu, F. Gao, W. Wang and W. Liu, *ACS Appl. Mater. Interfaces*, 2015, **7**, 8114-8124.
35. X. Zhang, K. Zhang and R. Haag, *Biomater. Sci.*, 2015, **3**, 1487-1496.
36. Y. Lee, S. Fukushima, Y. Bae, S. Hiki, T. Ishii and K. Kataoka, *J. Am. Chem. Soc.*, 2007, **129**, 5362-5363.
37. J. Z. Du, X. J. Du, C. Q. Mao and J. Wang, *J. Am. Chem. Soc.*, 2011, **133**, 17560-17563.
38. J. J. Chen, J. X. Ding, Y. Zhang, C. S. Xiao, X. L. Zhuang and X. S. Chen, *Polym. Chem.*, 2015, **6**, 397-405.
39. S. S. Han, Z. Y. Li, J. Y. Zhu, K. Han, Z. Y. Zeng, W. Hong, W. X. Li, H. Z. Jia, Y. Liu, R. X. Zhuo and X. Z. Zhang, *Small*, 2015, **11**, 2543-2554.
40. A. E. Baydar, V. G. Boyd, J. Aupers and P. F. Lindley, *J. Chem. Soc., Perkin Trans. 1*, 1981, 2890-2894.
41. R. Murali, H. S. P. Rao and H. W. Scheeren, *Tetrahedron*, 2001, **57**, 3165-3174.
42. G. Piizzi and M. E. Jung, *Chem. Rev.*, 2005, **105**, 1735-1766.
43. Z. J. Zhang, X. Zhang, X. H. Xu, Y. Li, Y. Li, D. Zhong, Y. He and Z. Gu, *Adv. Funct. Mater.*, 2015, **25**, 5250-5260.
44. S. Kang, Y. Kim, Y. Song, J. U. Choi, E. Park, W. Choi, J. Park and Y. Lee, *Bioorg. Med. Chem. Lett.*, 2014, **24**, 2364-2367.
45. A. J. Kirby and P. W. Lancaster, *J. Chem. Soc., Perkin Trans. 2*, 1972, **2**, 1206-1214.
46. H. Park, J. Suh and S. Lee, *J. Mol. Struct. Theochem.*, 1999, **490**, 47-54.
47. J. Cai and Z. J. Wu, *J. Theor. Comput. Chem.*, 2009, **8**, 1217-1226.
48. M. Dror and M. Levy, *J. Polym. Sci.*, 1975, **13**, 171-187.
49. J. E. T. Corrie, M. H. Moore and G. D. Wilsonb, *J. Chem. Soc., Perkin Trans. 1*, 1996, **8**, 777-781.
50. K. Maier and E. Wagner, *J. Am. Chem. Soc.*, 2012, **134**, 10169-10173.
51. S. A. Jacques, G. Leriche, M. Mosser, M. Nothisen, C. D. Muller, J. S. Remy and A. Wagner, *Org. Biomol. Chem.*, 2016, **14**, 4794-4803.
52. X. Liu, J. Zhang and D. M. Lynn, *Soft Matter*, 2008, **4**, 1688-1695.

Graphics for TOC



Controlled synthesis and in-depth study on pH-dependent hydrolysis profiles of substituted maleamic acid derivatives.